Measurement of Attachment-Line Location in a Wind-Tunnel and in Supersonic Flight

Naval K. Agarwal[†], Stan J. Miley [¶], Michael C. Fischer [‡] NASA Langley Research Center Hampton, VA 23665

and

Bianca T. Anderson* and Robert J. Geenen* NASA Dryden Flight Research Facility Edwards, CA 93523

Abstract

As a part of the supersonic laminar flow control research program, experiments are being conducted to measure the attachment-line flow characteristics and its location on a highly swept aircraft wing. Initially, subsonic wind tunnel tests were performed on two-dimensional models to develop sensors and techniques for the flight application. The wind tunnel test results suggest that, under certain conditions at the leading edge there are low frequency streamwise velocity fluctuations present in the laminar boundary layer which undergo a phase change at the stagnation Therefore, if present in flight, this distinct change in phase, i.e., time shift of signals from either side of the stagnation po st

All other rights are reserved by the copyright

owner.

The phase-reversal phenomenon was examined to determine the attachment-line location on a highly swept wing. Test results indicate that the phase-reversal phenomenon may not be applicable in flight. Additional data analyses is continuing to account for phase differences introduced by the recording system. A final determination on the existence of phasereversal in flight will require the results of further analysis and possibly additional flight testing. Some representative attachment-line data are presented and discussed as well as the results from the wind tunnel investigation.

Nomenclature

point, can be used to determine the stagnation-line or attachment-line location.	DFRF	NASA/Dryden Flight Research Facility
	HLFC	Hybrid Laminar-Flow Control
† Senior Scientist, AS&M, Inc., Associate		
Fellow AIAA	HSCT	High Speed Civil Transport
¶ Senior Research Associate, NRC, Member AIAA	LaRC	NASA (Longley Degearch Center
‡ F-16XL SLFC Technical Manager,	Lanc	NASA/Langley Research Center
LFCPO/FAD, Member AIAA	LFC	Laminar Flow Control
*Aerospace Engineer, Member AIAA		
-	M	Mach Number
Copyright © 1992 by the American Institute		
of Aeronautics and Astronautics, Inc. No	NASA	National Aeronautics and Space
copyright is asserted in the United States		Administration
under Title 17, U.S. Code. The U.S.		
Government has a royalty-free licence to exercise all rights under the copyright	U_{∞}	Free-stream tunnel velocity
claimed herein for Governmental purposes.	Re	Reynolds number

Introduction

In a joint Boeing and National Aeronautics and Space Administration (NASA) program, extensive flight tests on a Boeing-757 using hybrid laminar-flow control (HLFC) have shown that a significant amount of laminar flow can be achieved at subsonic speeds. laminar-flow control (LFC) is also a potential high-payoff technology for the High Speed Civil Transport (HSCT). Therefore, NASA has initiated a program to determine the feasibility of achieving extensive laminar flow on a highly-swept wing at supersonic speeds. The General Dynamics F-16XL was chosen as the test aircraft due to its possession of a double delta-wing planform representative of future HSCT's proposed by industry. Preliminary feasibility studies have shown that maintenance of laminar flow through active boundary-layer control is viable on the inboard (subsonic leading edge) section of this type of wing planform. There are two F-16XL aircraft currently involved in supersonic laminar-flow research at the NASA Dryden Flight Research Facility (DFRF). The F-16XL-1 has a single-place cockpit (see figure 1) while the F-16XL-2 has a dual-place cockpit. Current research activity at DFRF is utilizing the F-16XL-1 with a laminar-flow suction glove (figure 1) a co-operative Rockwell/NASA experiment designed to establish the feasibility of obtaining laminar flow on a supersonic highly swept wing and to provide data for CFD code calibration. The small dark area is the perforated titanium laminar flow suction glove (active), while the white area is a non-suction (passive) glove fairing. The F-16XL-2 will be used for flight research beginning July 1992. A leading-edge passive glove will be tested initially on the F-16XL-2 and will focus on providing both leadingedge physics information and data for code calibration.

The attachment line is the spanwise dividing line between upper-surface and lowersurface flow on the leading edge of swept wings. For unswept, i.e., straight wings, this line corresponds to the locus of stagnation points along the leading edge. However, for swept wings, there is no true stagnation point at the leading edge, due to a spanwise component of flow which is inherent with wing sweep. Knowledge of the accurate location of the attachment line is necessary to determine the state of the attachmentline boundary layer, which is of major importance since the local state of the attachment-line boundary layer is the starting point for the streamwise flow over the wing. If this boundary layer is laminar, then the streamwise flow boundary layer is initially laminar. However, if the attachment-line boundary layer is turbulent, then the streamwise flow will be turbulent also. To maintain laminar flow on a swept wing, the attachment-line boundary layer must remain laminar above a certain momentum-thickness Reynolds number. otherwise, once transition occurs, it contaminates the remaining spanwise part of the wing boundary layer with turbulence. Transition criteria for the attachment-line boundary layer indicate that for laminar flow, the attachment line should be maintained in the region of the leading edge with the highest degree of curvature. This again emphasizes the importance of determining its location in flight as accurately as possible.

During the initial phases of the suction glove experiment on the F-16XL-1, experience with pressure distribution measurements in the leading edge indicated that surface static pressure taps could not provide the necessary spatial resolution or accuracy needed to precisely determine the attachment line location. Because of the thin boundary layer at supersonic speeds and the high surface curvature at the leading edge, pressure orifice interference appeared to have a pronounced effect on the scatter of the data to the extent that the interpolating process necessary to locate the attachment line became highly questionable. Therefore, a new technique to measure the attachmentline location on the F-16XL-1 glove using an array of closely spaced hot-film sensors flush mounted on the wing leading edge, was investigated.

Wind-tunnel tests were conducted on twodimensional models, i.e., a cylinder and an airfoil to develop sensors and measurement techniques for the flight application. This study looked at the phase reversal across the leading-edge stagnation point as a possible means to determine the location of the stagnation point. Wind tunnel tests indicated, as discussed in the following section, that the existence of a lowfrequency disturbance is important in the use of the phase-reversal technique. Mangalam and Kubendran 1 indicated a direct coupling between the dominant frequencies of flow oscillations at the leading edge, laminar-separation unsteadiness, and vortex shedding. influence of cylindrical-body wake oscillations on the pressure field and associated feedback mechanism have also been discussed by Morkovin². studied the character and origin of the different components which make up the noise signature of a wing. Paterson et al.4 show that the condition necessary for the tonal behavior to exist is that the wing must be totally laminar. The tone originates from discrete vortex shedding accompanies the breakdown of a laminar wake. Paterson et al. concluded that the discrete tonal behavior disappears, with the appearance of a turbulent boundary layer. Phase reversal in the signal from sensors located across a laminar separation bubble was observed by Stack et al.⁵ on low Reynolds number airfoils. Scott et al.6 observed a phase reversal in hot-film sensors across the stagnation location on an airfoil using the same wind tunnel as used in the present investigations. Mangalam et al. 7 also indicated the presence of phase reversal from sensors across the attachment line on a swept wing in wind-tunnel tests.

This paper will describe in detail, the results of subsonic wind-tunnel tests on a cylinder and an airfoil model, and preliminary results from flight tests at supersonic conditions.

Test Apparatus

The ground experiments were performed in the 12- by 17-inch test section of the

Velocity Calibration Wind Tunnel at the Instrument Research Division of the Langley Research Center. This wind tunnel can reach test-section flow speeds up to 85 m/sec and has a turbulence level ranging between 0.7% at low speeds to 0.3% at higher speeds. A 50 hp motor drives a squirrel cage blower at one of two selectable speeds. The test section velocity is controlled by opening and closing 12 radial damper vanes located downstream of the diffuser, and changing the motor speed. The wind tunnel is shown schematically in figure 2. More details of the wind tunnel and the test section are contained in ref. 8.

Two models used were a circular cylinder (diameter 101mm), and a NACA 0012 airfoil (chord 255mm). Surface-mounted microthin hot-film sensor arrays were wrapped around the leading edge of the cylinder and the airfoil model. Surface-mounted multielement hot-films have been utilized at NASA Langley Research Center to study the boundary-layer state, transition, and separation for both the subsonic and supersonic regimes 6-10. These sensors are formed by vapor deposition of nickel and copper on a 50 micron thick Kapton Sheet. The Kapton sheet is glued (about 20 micron thick) to models and provides nearly nonintrusive surface based measurements. A 33-element sensor array (sensor size: 1.145mm x 0.125mm, and spacing 0.77mm) was used on the leading edge of both models. A 50-element sensor array with spacing of 1.52 mm was also used near the trailing edge of the airfoil model covering X/C of 0.6 to 0.9. Flat ribbon cables were soldered to copper leads (laid on the same Kapton sheet as the sensors) from each sensor and routed through ports on the models. Care was taken to ensure that the connecting wires did not interfere with the flow at the test regions. DISA 55M10/55M12 constant temperature anemometer bridges were used to operate the sensors. The sensors were uncalibrated and were operated at an overheat ratio of 1.3. The models were mounted on a circular plate attached to the wind-tunnel floor, which could be rotated by an external screw mechanism to vary the angle-of-attack. The cylinder model and the wing instrumented

with hot-film sensor arrays, are shown in figures 3 and 4, respectively.

The F-16XL test vehicle planform consists of a inboard section with a sweep of 70 degrees and a outboard section with a sweep of 50 degrees. The NASA supersonic laminar flow research program and the aircraft are described in more detail by Fischer and Vemuru¹¹. A 20-element hot-film array (sensor size: 1.145mm x 0.125mm) with a sensor spacing of 0.0286 inch, was wrapped around the leading edge just inboard of the active glove as shown in figures 5 and 6. Care was taken to maintain wrinkle-free installation of the sensor array due to the sharp leading edge and surface curvature near the leading edge. Due to the large variations in the temperatures associated with altitudes and compressibility, the hotfilm sensors were operated with a temperature compensated anemometer system described in ref. 12. This anemometer system utilizes a second hotfilm array to measure the instantaneous local temperature. This temperature signal is utilized by the anemometer circuit to adjust the sensor overheat. The temperature sensors are at the same chord location as the flow sensors, and are located about 1.5 inches in spanwise direction from the flow sensor array: refer to figure 6. Due to the limited number of anemometers which could be accommodated onboard, only 12 sensors (5 through 15; see figure 7) were used. The sensor output was recorded on an onboard 14 track FM tape recorder. The tape recorder was operated at 15 inch/sec., which resulted in a frequency response of 10 kHZ. from the sensors. Time code was recorded on one channel of the recorder which was later used in digitization of the data.

Results and Discussion

Wind Tunnel Investigations:

The results from the cylinder model were consistent with those of Mangalam and Kubendran¹. A tonal signal in the flow at the stagnation line was observed as long as the cylinder was subcritical, i.e., laminar separation aft of maximum thickness. Using a tuft it was observed that as the flow

changed from subcritical to supercritical. i.e., laminar separation being replaced by transition to turbulence and subsequent turbulent separation, the tone disappeared. A spectrum from one of the sensors showing this is given in figure 8. A phase reversal in this tonal signal was observed at the stagnation line. Figure 9 shows time histories of six sensors band-pass filtered for the tonal signal. Phase reversal occurs between sensors 4 and 5 indicating that the stagnation line lies between these two sensors. The location of the stagnation line was confirmed by surface pressure measurements. In addition, by comparing phase relationships between sensors on the same side of the cylinder, waves propagating in the boundary layer upstream from the rear of the cylinder were also observed. Rotating the cylinder moved the phasereversal effect through the sensor array accordingly so that the location of the stagnation line was consistent with angle setting.

In addition to the tonal signal, phase spectra of the sensor signals showed a broadband phase reversal over the low frequency range. This was particularly evident for supercritical flow where the tonal signal was absent. Figure 10 shows a phase spectrum corresponding to the condition of figure 9. The tonal signal lies within the frequency band of phase reversal, but otherwise can not be distinguished from other sources. Figures 11 and 12 show amplitude and phase spectra for a supercritical flow case where the tonal signal is not present. Phase reversal is present, but no discrete source is identifiable. A consistent time history, as shown in figure 8, was not found.

The broadband phase reversal pointed to other aerodynamic sources besides the vortex shedding of the cylinder. A hot-wire probe was installed in the test section and the test condition repeated. Spectra of flow disturbances in the tunnel were obtained; an example of which is given in figure 13. It is seen to compare with the spectra of the cylinder hot-film sensors of figures 8 and 11. It was evident that the wind tunnel was supplying an aerodynamic disturbance of

sufficient strength to produce a phasereversal signal at the stagnation line of the model.

The behavior of the airfoil was different from the cylinder in that no self-generated aerodynamic disturbance, i.e., vortex shedding was present. Detailed measurements on the airfoil model indicated that in the present set-up it was possible to obtain laminar flow on one side of the airfoil model only. Paterson et al. 4 showed that for a tonal signal to exist, the wing must be totally laminar. Achieving laminar flow on both sides of the airfoil was not possible, even at the low Reynolds number of the test, due to presence of the sensor connecting leads on the wing. Also, such extensive laminar flow is not likely to exist in flight experiments. Except for the absence of the vortex shedding signal, the amplitude spectra were similar to those of the cylinder. An example is given in figure 14. Random disturbances in the tunnel flow interacting with the wing leading edge, with intensity increasing with the angle-ofattack, provided a signal necessary for the application of the phase-reversal technique. The stagnation line location was easily identifiable by phase reversal between adjacent sensors. A representative phase spectrum for this is shown in figure 15. The location of the stagnation line as indicated by phase reversal was consistent with that indicated by pressure distribution measurements and extended over a wide range of angles-of-attack.

The results of the wind tunnel test showed that the stagnation line could be located by looking for phase reversal between adjacent hot-film sensors. However, this technique is dependent on the presence of an aerodynamic disturbance. For the technique to be of practical use, this disturbance must be known to exist a priori.

Flight Investigations:

A preliminary investigation of the existence of a suitable aerodynamic disturbance and possible use of the phase-reversal technique was carried out on the F-16XL aircraft. It was assumed that a suitable

aerodynamic disturbance might exist associated with shock formation in supersonic flight. The results from the wind tunnel tests showed that a disturbance was necessary, but gave no assurance that one would be encountered in flight. The flight investigation relied on the possible existence of a disturbance associated with the shock structure. As this was the first time that such high-frequency flow sensors had been located on the leading edge and flown at supersonic speeds, there was no data from previous work to fall back on regarding the possibility of such a disturbance.

The aircraft was flown through a series of test conditions for which laminar flow was known to exist. With the present configuration, laminar flow can only be obtained at angles-of-attack below the corresponding trim angles for the test matrix of Mach numbers and altitudes. This results in pitch-over maneuvers being required to reach the test matrix points, leading to transient conditions and small data windows.

In all the test conditions flown, no consistent phase-reversal behavior was found. Analyses of the leading-edge hot-film sensor signals from the F-16XL aircraft show a complicated flow pattern. Unlike the wind-tunnel tests, a true attachment line exists here. The flow is laminar or turbulent depending upon local values of attachmentline momentum-thickness Reynolds numbers. Figure 16 shows a representative time history of selected leading-edge sensors as the aircraft is maneuvered through a range of angles-of-attack. Figures 17 and 18 show the corresponding angle-ofattack and Mach number time history. The turbulence level from sensor 10 has been added to the curve in figure 17 so that correlation between leading-edge flow state and angle-of- attack can be seen. At anglesof- attack less than 3 degrees, the leadingedge flow is laminar. Between 3 and 5 degrees, the leading-edge flow is turbulent. This is due to the attachment line moving below the leading edge with increasing angle-of-attack. The radius of curvature of the surface increases leading to an increase

in the momentum-thickness Reynolds number which causes transition in the attachment line and subsequent turbulent flow. At angles-of-attack above 5 degrees, the strong favorable pressure gradient at the leading edge causes the boundary-layer flow to relaminarize as it progress to the upper surface. The lower surface flow becomes turbulent above 5 degrees due to increasing momentum-thickness Reynolds number. A demarcation between upper surface flow and lower surface flow is apparent in figure 16. The turbulence grows from the attachment line. For the range of angles-of-attack shown in figure 17 the attachment line traverses through the entire sensor array on the leading edge. This movement of attachment line is not obvious from figure 16, but the effect of movement is seen in the laminar and turbulent regions.

As stated before, a consistent behavior of phase reversal in the signals from the leading-edge hot-film sensors was not seen in these first exploratory flights. As seen from the wind-tunnel results, in the case of an airfoil, the phase shift is not evident from the time-histories and the spectral analysis of the signal is necessary. But, since the data were recorded on a tape recorder and also the data analysis process requires digitizing the signals from a copy of the original FM flight data tape, each analog tape recorder in this process may introduce phase shifts between the respective data channels. Additional analysis of the data, to include any such phase shift introduced, will be required before a final determination on the existence of phase reversal can be made. It is planned to investigate the flow further outboard on the wing in future flights before a decision is made regarding the usefulness of the phase-reversal technique for supersonic flight.

<u>Acknowledgements</u>

The authors acknowledge the help of microelectronics and technical support section of electronics technology branch, LaRC in fabricating the sensors, and the F-16XL technical staff at DFRF for performing the flight tests.

References

- Mangalam, S.M., and Kubendran, LK., "Experimental Observations on the Relationship Between Stagnation Region Flow Oscillations and Eddy shedding for Circular Cylinder," ICASE/NASA LaRC Instability Workshop, NASA Langley Research Center, 1989, pp. 3 72-386.
- Morkovin, M.V., "Recent Insights into Instability and Transition to Turbulence in Open-Flow Systems," AIAA Paper No. 88-3685, 1988.
- ³ Tam, C.K.W., "Discrete Tones of Isolated Airfoils," Journal of the Acoustical Society of America, Vol. 55, No. 6, June 1974, pp. 1173-1177.
- ⁴ Paterson, R.W., Vogt, P.G., and Fink, M.R., "Vortex Noise of Isolated Airfolls", Journal of Aircraft, Vol. 10, No. 5, May 1973, pp. 296-302.
- ⁵ Stack, J.P., Mangalam, S.M., Berry, S.A., "A Unique Measurement Technique to Study Laminar-Separation Bubble Characteristics on an Airfoil", AIAA Paper No. 88-3675, 1988.
- ⁶ Scott, M. A., Carraway, D.L., and Lee, C.C., "A Comparison of Techniques for the Determination of Stagnation Location," The 14th International Congress on Instrumentation in Aerospace Simulation Facilities, Rockville, MD, October 27-31, 1991.
- Mangalam, S.M., Maddalon, D.V., Saric, W.S., and Agarwal, N.K., "Measurements of Crossflow Vortices, Attachment-Line Flow, and Transition using Microthin Hot Films," AIAA Paper No. 90-1636, 21st Fluid Dynamics, Plasma Dynamics and Lasers Conference, Seattle, WA, June 18-20, 1990.
- ⁸ Wusk, M.S., Carraway, D.L., and Holmes, B.J., "An Arrayed Hot-Film Sensor for Detection of Laminar Boundary-Layer Flow Disturbance Spatial Characteristics," AIAA Paper No. 88-4677-CP, AIAA/NASA/AFWAL Sensors & Measurements Technologies

Conference, Atlanta, GA, September 7-9, 1988.

⁹ Holmes, B.J., Carraway, D.L., Manuel, G.S., and Croom, C.C., "Advanced Measurement Techniques", Proceedings of Research in Natural Laminar Flow and Laminar Flow Control, NASA CP-2487, 1987.

10 Agarwal, N.K., Maddalon, D.V., Mangalam, S.M., and Collier, F. S., Jr., "Cross-Flow Vortex Structure and Transition Measurements using Multi-Element Hot Films," AIAA Paper No. 91-0166, 29th Aerospace Sciences Meeting, Reno, NV, January 7-10, 1991

11 Fischer, M. C., and Vemuru, C.S., "Application of Laminar Flow Control to the High Speed Civil Transport - The NASA Supersonic Laminar Flow Control Program," SAE Paper No. 912115, Aerospace Technology Conference and Exposition, Long Beach, CA, September 23-26, 1991.

12 Chiles, H., R., and Johnson, J. B., "Development of a Temprature-Compensated Hot-Film Anemometer System for Boundary-Layer Transition Detection on High-Performance Aircraft," NASA TM-86732, 1985.

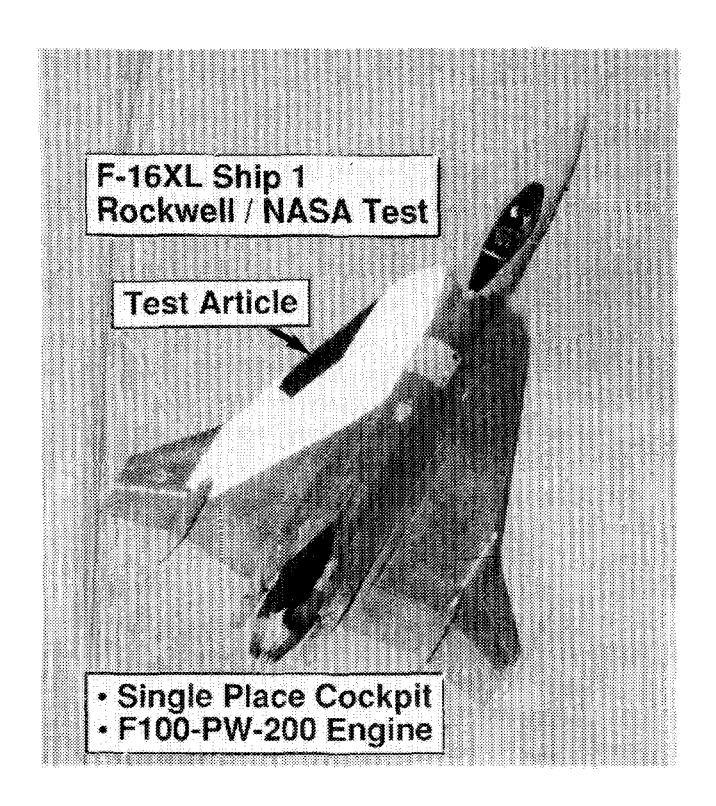


Figure 1: F-16XL-1 aircraft.

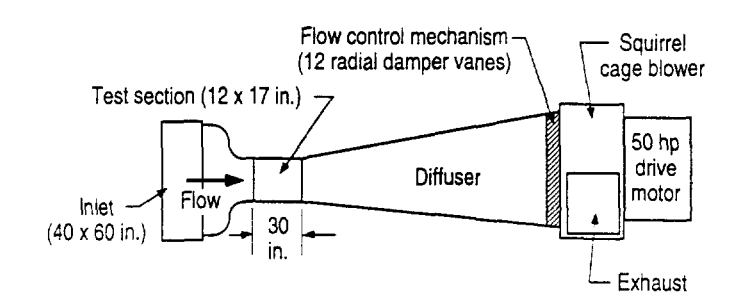


Figure 2: Schematic of Velocity Calibration Wind-Tunnel of Instrument Research Division at Langley Research Center.

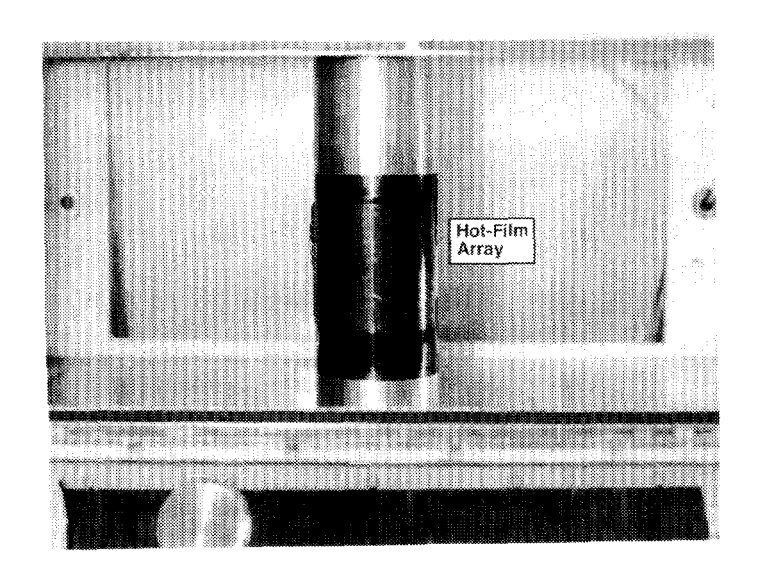


Figure 3: Cylinder model in wind-tunnel.

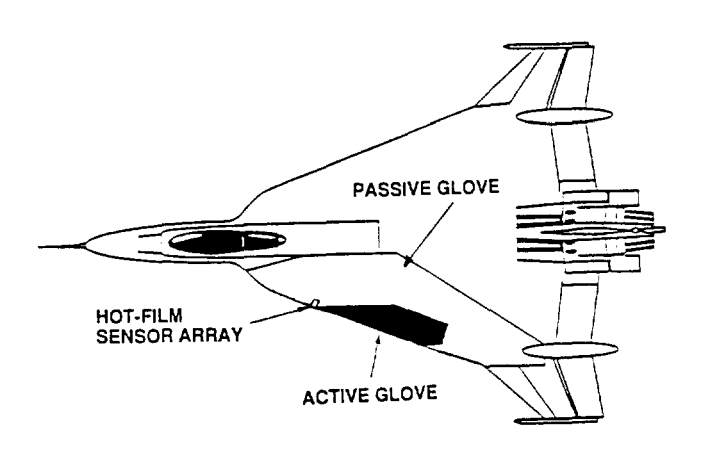


Figure 5: Location of hot-film sensor array on the F-16XL-1 aircraft.

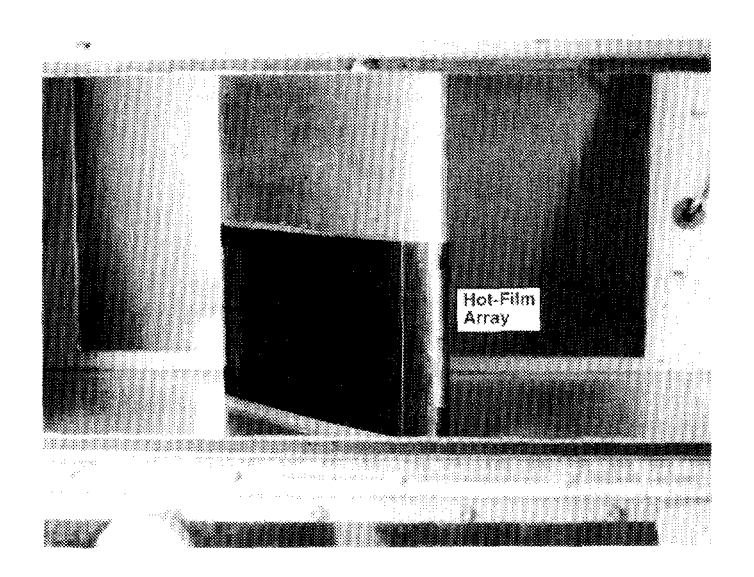


Figure 4: Airfoil model in wind-tunnel.

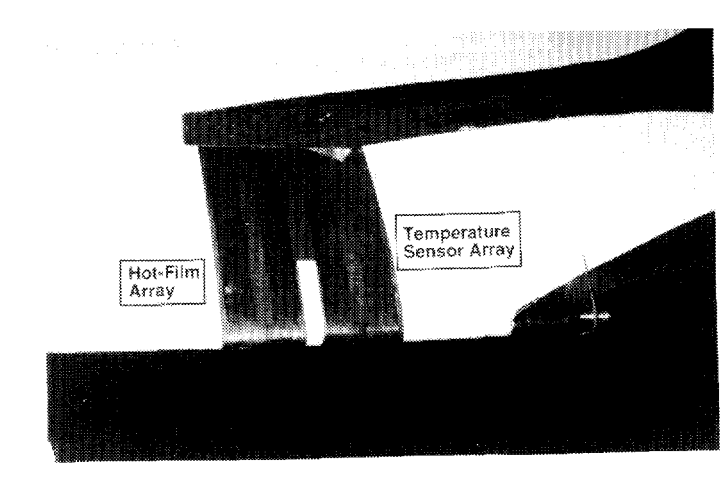


Figure 6: Close-up view of hot-film sensor array on the F-16XL-1 aircraft.

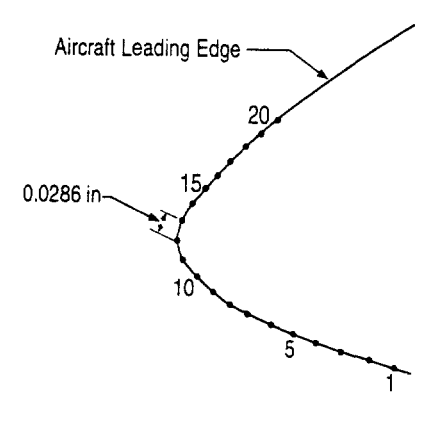


Figure 7: Location of hot-film sensors on the leading edge (not to scale).

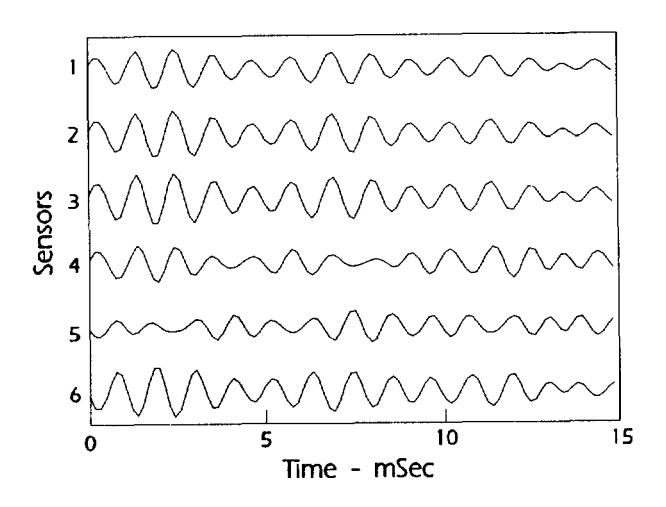


Figure 9: Time-histories of hot-film signals located across the stagnation-line of cylinder model.

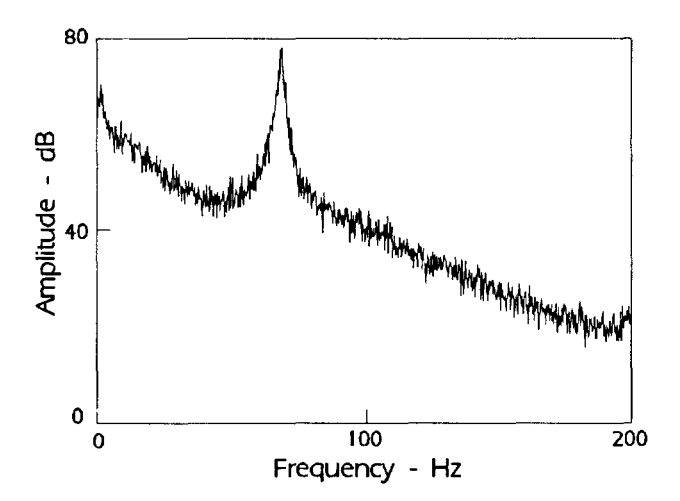


Figure 8: Power spectral density of hot-film signal (sensor 4 of figure 9); cylinder model, $R_e = 2.33 \times 10^5$.

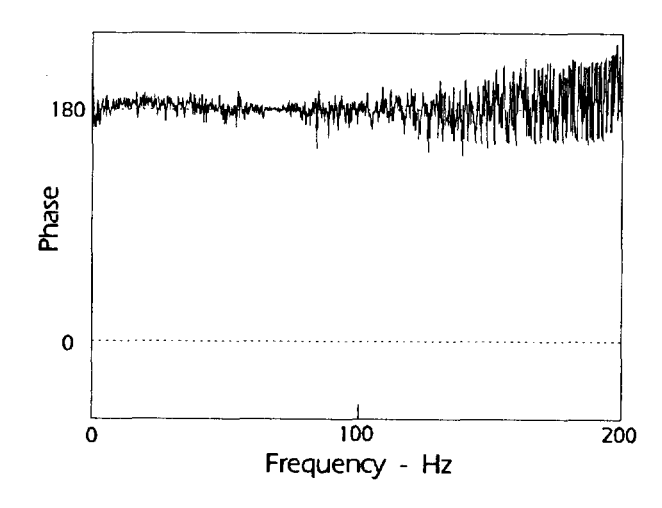


Figure 10: Phase spectrum of hot-film sensors 4 and 5 of figure 9.

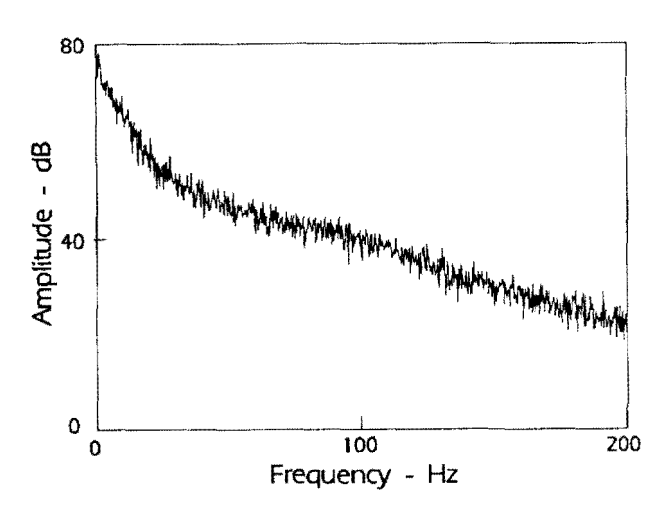


Figure 11: Power spectral density of hot-film signal (sensor 4 of figure 9) for supercritical case, $R_e = 3.36 \times 10^5$.

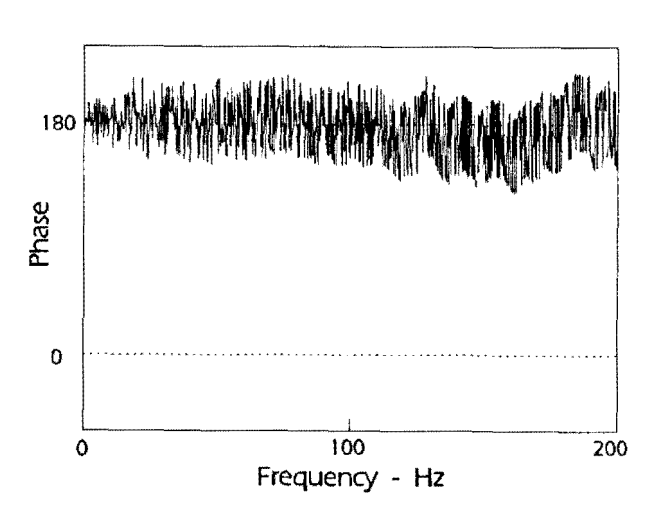


Figure 12: Phase spectrum of hot-film signals (sensors 4 and 5 of figure 9) for supercritical case.

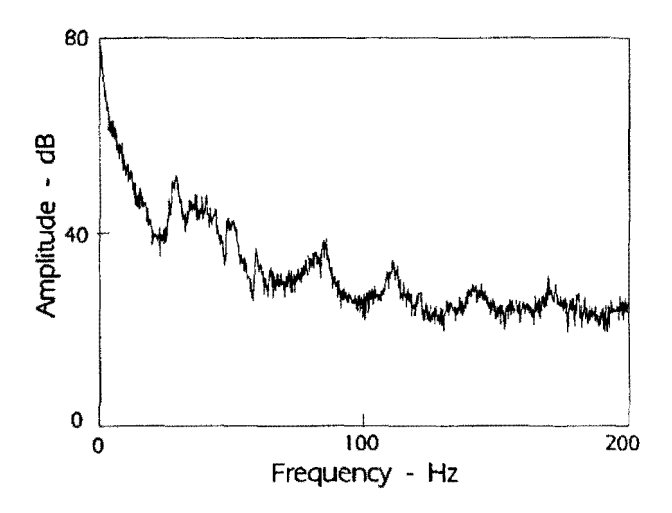


Figure 13: Power spectral density of hot-wire signal; tunnel free-stream, $U_{\infty} = 42.6$ m/sec.

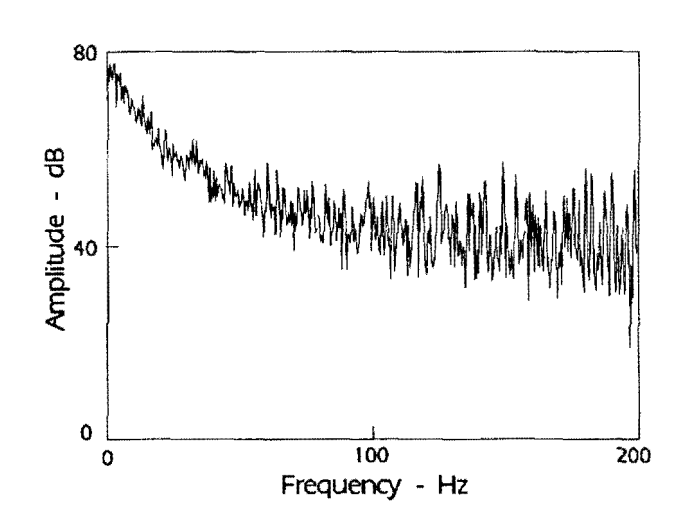


Figure 14: Power spectral density of hot-film signal; airfoil model, $R_e = 7.31 \times 10^{5}$, $\alpha = 0$ degrees.

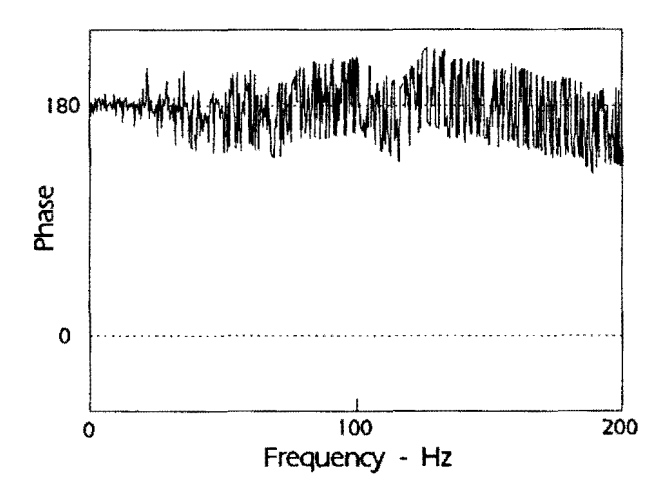


Figure 15: Phase-spectrum of hot-film signal; airfoil model.

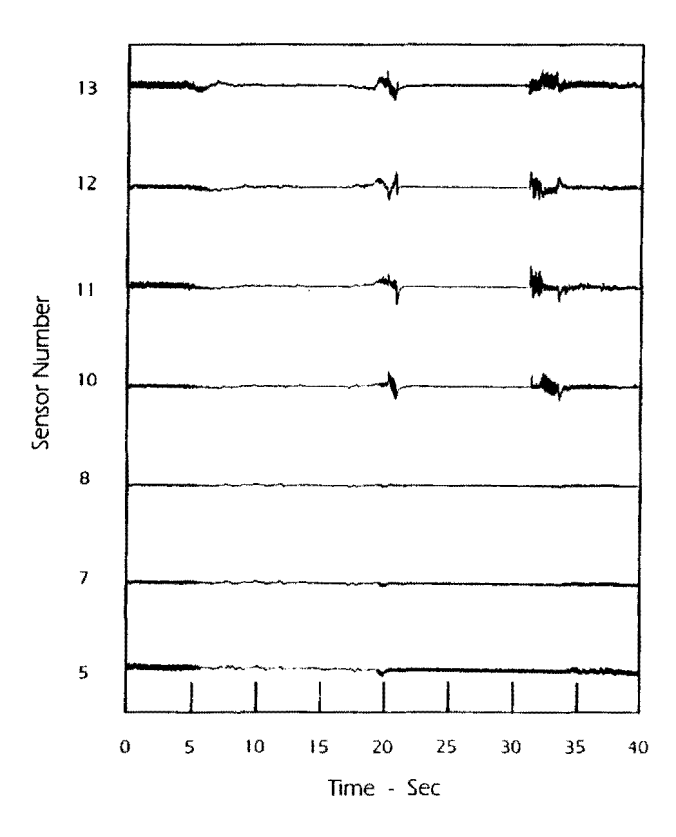


Figure 16: Time-histories of hot-film signals from F-16XL-1 leading-edge sensors.

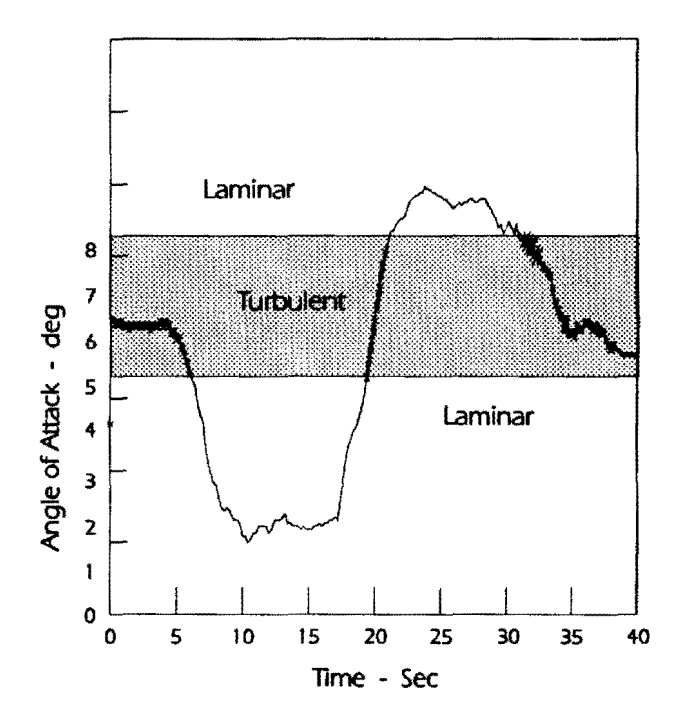


Figure 17: Angle-of-attack, a variation for the case shown in figure 16.

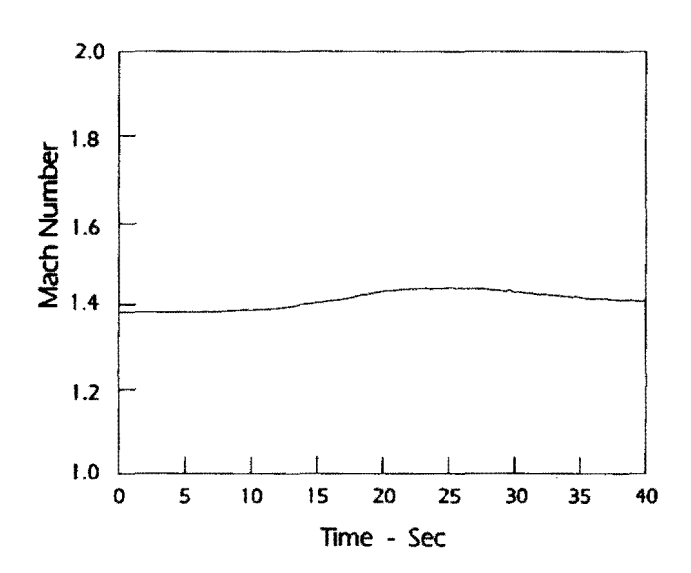


Figure 18: Mach Number variation for the case shown in figure 16.